Non-Abelian Aharonov-Bohm scattering of spinless particles

M. Gomes, L. C. Malacarne,* and A. J. da Silva
Instituto de Física, Universidade de São Paulo, Caixa Postal 66318 - 05315-970, São Paulo - SP, Brazil
(Received 16 July 1998; published 25 January 1999)

The Aharonov-Bohm scattering for spinless, isospin 1/2, particles interacting through a non-Abelian Chern-Simons field is studied. Starting from the relativistic quantum field theory and using a Coulomb gauge formulation, the one loop renormalization program is implemented. Through the introduction of an intermediary cutoff, separating the regions of high and low integration momentum, the nonrelativistic limit is derived. The next to leading relativistic approximation is also determined. In this approach quantum field theory vacuum polarization effects are automatically incorporated.
[S0556-2821(99)04002-3]

PACS number(s): 11.10.Kk, 11.10.Gh

I. INTRODUCTION

A great deal of interest has been devoted in recent years to the study of the Aharonov-Bohm (AB) effect, the scattering of charged particles by an impenetrable magnetic flux tube [1]. This situation was motivated both by potential applications, which come from many different areas, and also by some conceptual difficulties found in the AB scattering of spinless particles. In that case, the Born approximation failed to reproduce the expansion of the exact result and, furthermore, the second Born approximation turned out to be divergent [2]. These issues have been investigated considering as equivalents the AB effect and the scattering of particles interacting through a Chern-Simons (CS) field. In a nonrelativistic context, it was shown that, up to one loop, that is, the second Born approximation, agreement of the perturbative calculation with the expansion of the exact result could be achieved by introducing an extra quartic self-coupling of the scalar particles [3] tuned to eliminate divergences and restore the conformal invariance of the tree amplitude. For the scattering of two spin up fermions it was verified [7] that an additional self-interaction was not needed since its role was provided by Pauli's magnetic term, in accordance with an earlier conjecture [3]. However, if the fermions had antiparallel spins the effect of the magnetic interaction canceled and a divergence showed up.

From a more basic standpoint, one can start directly from a relativistic quantum field theory of charged particles interacting through a CS field and then appropriately taking a nonrelativistic limit. Proceeding in this way, purely quantum field theory effects as vacuum polarization and anomalous magnetic moment are automatically incorporated. Such a procedure was applied successfully to the study of the AB scattering for both spin 0 and spin 1/2 particles [4,5]. The calculation was greatly facilitated by the introduction of an intermediary auxiliary cutoff which, in the Feynman integrals, separates the regions of high and low energy. This allows a direct simplification of the integrands and it is closely related to the methods of effective field theories [6]. For the case of spinless or antiparallel spin fermionic particles, it was found that the low energy part of the amplitude contains a logarithmic divergence in the limit of very high intermediary cutoff. Nevertheless, different from the nonrelativistic calculations previously mentioned, without any additional hypothesis, the needed counterterm is automatically afforded by the high energy part of the contribution. Besides that, terms absent from the direct nonrelativistic calculation were determined. These new interactions come from the high energy part of the amplitudes and modify in an essential way basic properties of the nonrelativistic scattering.

In this work we want to pursue these investigations by considering the non-Abelian AB effect for spinless particles, which corresponds to the problem of particles without spin but carrying isotopic spin scattered by an isotopic magnetic flux tube. Cosmic strings and black holes are the more natural applications of this subject [8].

The non-Abelian AB situation was first analyzed in a celebrated paper on nonintegrable phase factors [9] and since then it has been more quantitatively investigated at the quantum mechanical level [10]. Recently, in a direct nonrelativistic approach, the scattering has been discussed using a non-Abelian Chern-Simons field to simulate the flux tube with results similar to the ones mentioned above for the Abelian case [11,12]. Here we want to begin from a relativistic formulation which, as said before, already embodies radiative corrections. In this way we will be able to find next to leading corrections to the results presented in [11].

We will assume that the basic particles carry isotopic spin 1/2. In the language of the $2+1$ quantum field theory our system is described by the Lagrangian density [13]

$$\mathcal{L}=-\Theta\varepsilon^{\alpha\beta\gamma}\,\mathrm{tr}\left(A_\alpha\partial_\beta A_\gamma+\frac{2g}{3}A_\alpha A_\beta A_\gamma\right)+(D_\mu\Phi)^\dagger(D^\mu\Phi)-m^2\Phi^\dagger\Phi-\frac{\lambda_1}{4}(\Phi^\dagger\Phi)^2-\frac{\lambda_2}{4}(\Phi^\dagger T^a\Phi)^2, \tag{1}$$

where $D_\mu=\partial_\mu+gA_\mu$ is the covariant derivative and A^μ

*Permanent address: Departamento de Física, Universidade Estadual de Maringá - Av. Colombo, 5790 - 87020-900, Maringá -PR, Brazil.

$=A^{\mu}{}_{a}T^{a}$ and T_a are the generators of the group SU(2). As we shall see, up to one loop, the leading contributions correctly reproduce the nonrelativistic results whereas the next to leading contributions are new corrections to the nonrelativistic calculation. As we are mainly interested in the nonrelativistic limit, in this work we will employ a strict Coulomb gauge.

Our work is organized such that in Sec. II the nonrelativistic theory is briefly considered. We do that not only to fix our notation but also to make easier the comparison with the results of the nonrelativistic limit of Eq. (1). In Sec. III, after discussing the one loop renormalization program for the relativistic model, we analyze the two body scattering up to next to the leading nonrelativistic approximation. Final comments and a discussion of our results are presented at the end of that section.

II. THE NONRELATIVISTIC MODEL

In this section we want to summarize the results of the non-Abelian AB scattering of spinless particles. To facilitate comparison, we shall use essentially the same notation as in [11], but to keep contact with the results to be derived in the next section, we will employ a cutoff to regularize the spatial part of the loop integrals instead of dimensional regularization as it was done in that reference. The Lagrangian density which specifies the model is

$$\begin{aligned}\mathcal{L}_{NR}=&-\Theta\varepsilon^{\alpha\beta\gamma}\,\mathrm{tr}\left(A_{\alpha}\partial_{\beta}A_{\gamma}+\frac{2g}{3}A_{\alpha}A_{\beta}A_{\gamma}\right)\\&+i\Phi^{\dagger}D_{t}\Phi-\frac{1}{2m}(\mathbf{D}\Phi)^{\dagger}(\mathbf{D}\Phi)\\&-\frac{1}{4}\Phi^{\dagger}_{n'}\Phi^{\dagger}_{m'}C_{n'm'nm}\Phi_{m}\Phi_{m}-\frac{1}{\xi}\,\mathrm{tr}(\nabla\mathbf{A})^{2}\\&-\eta^{*a}(\boldsymbol{\delta}_{\mathbf{ab}}\nabla^{2}+gf_{abc}\mathbf{A^{c}}\cdot\nabla)\,\eta^{b},\end{aligned}\tag{2}$$

where Φ is an n component complex field belonging to the fundamental representation of the SU(n) group. The generators of the Lie algebra of SU(n), denoted by T^a satisfy

$$[T^{a},T^{b}]=f_{abc}T^{c}\tag{3}$$

and are normalized such that

$$\mathrm{tr}(T^{a}T^{b})=-\frac{1}{2}\delta^{ab}.\tag{4}$$

With respect the constant matrix $C_{n'm'nm}$ we just assume that it has the most general form compatible with the invariance of the action under the SU(n) transformations [11].

We will use a graphical notation where the CS field, the matter field and the ghost field propagators are represented by wavy, continuous and dashed lines respectively. In the Coulomb gauge, obtained by letting $\xi\to 0$, the analytic expressions for these propagators are as follows.

CS field propagator:

$$D^{\mu\nu}_{ba}(k)=D^{\mu\nu}(k)\,\delta_{ba}=\frac{1}{\Theta}\varepsilon^{\mu\nu\lambda}\frac{\overline{k_{\lambda}}}{\mathbf{k}^{2}}\;\;\delta_{ba}\,,\tag{5}$$

where $\overline{k^{\mu}}=(0,\vec{k})$.

Matter field propagator:

$$D_{nm}(p)=D(p)\,\delta_{nm}=\frac{i}{p_{0}-\dfrac{\mathbf{p}^{2}}{2m}+i\epsilon}\;\;\delta_{nm}\,.\tag{6}$$

Ghost field propagator:

$$G_{ba}(p)=G(p)\,\delta_{ba}=\frac{-i}{\mathbf{p}^{2}}\;\;\delta_{ba}\,.\tag{7}$$

The vertices of the Feynman's diagrams are of five different types:

Trilinear CS–matter field vertices (p and p' are the momenta through the scalar lines at the vertex)

$$\Gamma^{a,0}_{nm}(p,p')=-g(T^{a})_{nm}\tag{8}$$

for the trilinear coupling involving A^0, and

$$\Gamma^{a,i}_{nm}(p,p')=-\frac{g}{2m}(T^{a})_{nm}(p+p')^{i}\tag{9}$$

for the coupling containing $A^i, i=1,2$.

Trilinear CS–ghost field vertex

$$\Gamma^{abc,i}(p,p')=-gf^{abc}p'^{i}.\tag{10}$$

Quadrilinear CS matter field vertex

$$\Gamma^{ab,ij}_{nm}(p,p')=-\frac{ig^{2}}{2m}[T^{a}T^{b}+T^{b}T^{a}]_{nm}g^{ij}.\tag{11}$$

Trilinear CS field vertex

$$\Gamma^{abc,\mu\nu\lambda}(p,p')=ig\Theta f^{abc}\varepsilon^{\mu\nu\lambda}.\tag{12}$$

Quadrilinear matter field vertex

$$\Gamma(p,p')_{m'n'mn}=\frac{-i}{2}C_{m'n'mn}\,.\tag{13}$$

Using these rules, the tree approximation to the direct scattering amplitude corresponds to the graphs in Figs. 1(a) and 1(b). In the center of mass frame it is given by

$$\mathcal{M}(\theta)=-\frac{C}{2}-i\frac{2\pi}{m}\Omega\;\;\cot(\theta/2),\tag{14}$$

where θ is the scattering angle and $\Omega=(-g^2/2\pi\Theta)\,T^a\otimes T_a$. We use a simplified notation introduced in Ref. [11], where isospin indices are omitted. Accordingly, if the incoming and outgoing particles have isospin (n,m) and (n',m') the total scattering amplitude for the process is given by

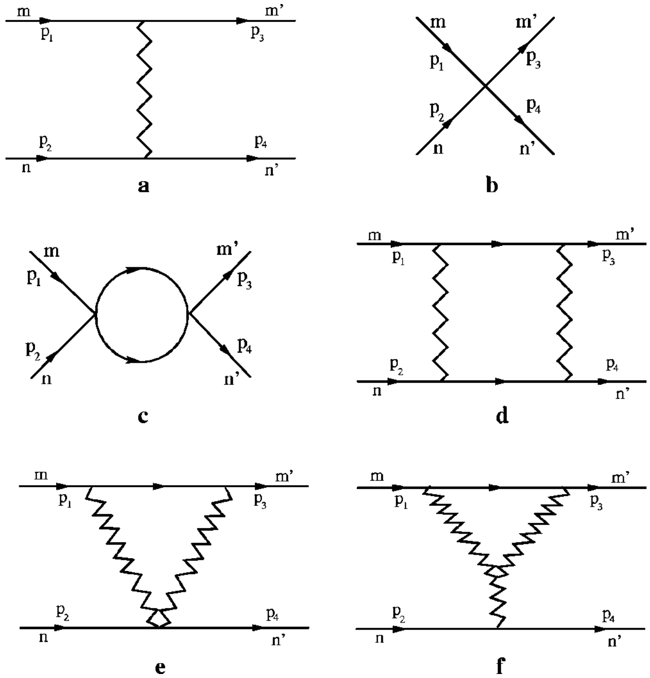

FIG. 1. Graphs contributing to the nonrelativistic scattering.

$$\mathcal{M}_{n'm';nm}(\theta)+(\theta\rightarrow\pi+\theta,n'\leftrightarrow m'), \tag{15}$$

where

$$\mathcal{M}_{n'm';nm}(\theta)=-\frac{C_{n'm'nm}}{2}+i\frac{g^2}{\Theta}T^a_{n'n}T^a_{m'm}\cot(\theta/2). \tag{16}$$

The one-loop graphs depicted in Figs. 1(c)–1(f) have been computed in [11] using dimensional regularization. Here we just quote the corresponding results obtained by introducing a cutoff Λ_{NR} in the spatial part of the loop integrals. We get

$$\mathcal{M}_c(\theta)=\frac{mC^2}{16\pi}\left[\log\left(\frac{\Lambda^2_{NR}}{\mathbf{p}^2}\right)+i\pi\right], \tag{17}$$

$$\mathcal{M}_d(\theta)=\frac{-\pi\Omega^2}{m}[2\log|2\sin(\theta/2)|+i\pi], \tag{18}$$

$$\mathcal{M}_e(\theta)=\frac{-\pi\Omega^2}{m}\left[\log\left(\frac{\Lambda^2_{NR}}{\mathbf{p}^2}\right)-2\log|2\sin(\theta/2)|\right]+\frac{g^2}{16m\Theta}\Omega\left[\log\left(\frac{\Lambda^2_{NR}}{\mathbf{p}^2}\right)-2\log|2\sin(\theta/2)|\right], \tag{19}$$

$$\mathcal{M}_f(\theta)=\frac{-g^2}{16m\Theta}\Omega\left[\log\left(\frac{\Lambda^2_{NR}}{\mathbf{p}^2}\right)-2\log|2\sin(\theta/2)|+1\right], \tag{20}$$

where $\mathcal{M}_i$ denotes the contribution coming from the graph i in Fig. 1. Note that the finite constant term in $\mathcal{M}_f$ can be absorbed into a redefinition of C. Afterwards, we see that our result agrees with Ref. [11] if the dimensional regularization parameter ϵ and our cutoff Λ_{NR} are related by

$$\frac{1}{\epsilon}+\ln\left(\frac{4\pi\mu^2}{\Lambda^2_{NR}}\right)-\gamma=0, \tag{21}$$

where γ is the Euler constant. Adding the above results and disregarding the mentioned constant term, we get

$$\mathcal{M}_{1loop}(\theta)=\frac{m}{16\pi}\left(C^2-\frac{16\pi^2\Omega^2}{m^2}\right)\left[\log\left(\frac{\Lambda^2_{NR}}{\mathbf{p}^2}\right)+i\pi\right]. \tag{22}$$

Thus, in complete analogy with what happens in the Abelian case, we now choose $C^2=16\pi^2\Omega^2/m^2$ to restore the conformal invariance of the tree approximation and reproduce the exact result

$$\mathcal{M}(\theta)=-i\frac{2\pi}{m}(\Omega\cot(\theta/2)-i|\Omega|), \tag{23}$$

as also derived by [11].

III. RELATIVISTIC THEORY

In the relativistic domain, the Feynman amplitudes are very intricate for a general matrix C. Considerable simplification occurs however if the gauge symmetry is taken as isospin SU(2) group [15]. Thus, for simplicity we restrict ourselves to the study of the SU(2) case described by the Lagrangian (1) where a gauge fixing and ghost terms must be added for a proper quantization.

Of course, we choose to work in a strict Coulomb gauge as before. As described below, unless by obvious modifica-

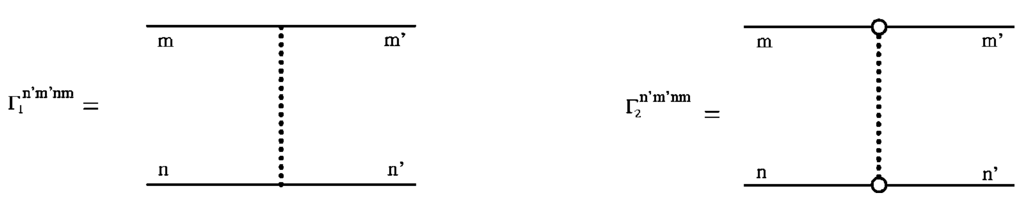

FIG. 2. Alternative graphical representation for the four scalar field vertex.

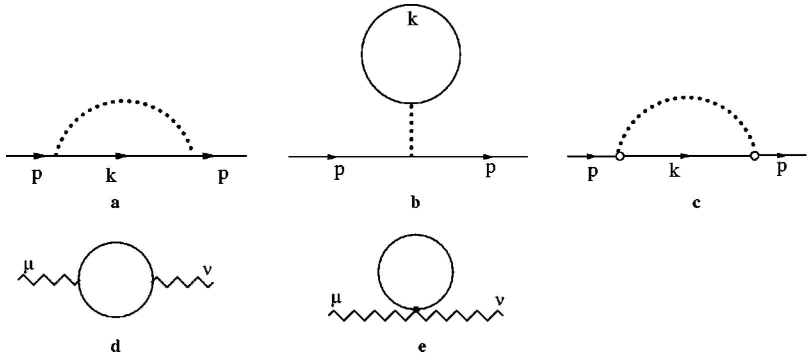

FIG. 3. One loop contributions to the matter field and CS self-energy.

tions the graphical representation of Feynman amplitudes are the same as before. However, as indicated in Fig. 2, to better clarify the matrix structure of the four scalar field vertices we will sometimes use an auxiliary dotted line whose corresponding propagator is just the identity. Concerning the free field propagators, we have to use the matter field relativistic propagator

$$\Delta_{nm}(p)=\Delta(p)\delta_{nm}=\frac{i}{p^2-m^2+i\epsilon}\ \delta_{nm} \tag{24}$$

instead of Eq. (6) whereas the CS free propagator continues to be given by Eq. (5). The new rules for the vertices are as follows.

Trilinear CS–matter field vertex

$$\Gamma^{a,\mu}_{nm}(p,p')=-g(T^a)_{nm}(p+p')^{\mu}. \tag{25}$$

Quadrilinear CS matter field vertex

$$\Gamma^{ab,\mu\nu}_{nm}(p,p')=-ig^2[T^aT^b+T^bT^a]_{nm}g^{\mu\nu}. \tag{26}$$

Quadrilinear matter field vertices

$$\Gamma_1^{n'm'nm}(p,p')=\frac{-i\lambda_1}{2}I^{n'n}I^{m'm} \tag{27}$$

for the vertex proportional to λ_1 (I denotes the identity matrix in the isospin space). We have also

$$\Gamma_2^{n'm'nm}(p,p')=\frac{-i\lambda_2}{2}(T^a)^{n'n}(T^a)^{m'm} \tag{28}$$

for the vertex proportional to λ_2. The CS–ghost field vertex and the trilinear CS field vertex are, up the replacements of f^{abc} by ϵ^{abc}, the same as before.

Before embarking into the discussion of the scattering process and its nonrelativistic limit we will examine the other one loop superficially divergent amplitudes. The Coulomb gauge CS theory without matter fields has been analyzed in Ref. [14] with the conclusion that there are no radiative corrections to the Green functions. For that reason we will restrict our study to graphs arising from the coupling to the scalar matter field.

We begin by considering the matter self-energy contributions whose nonvanishing contributions are in Figs. 3(a)–3(c). Because of the specific form of the CS field propagator or the trace over the SU(2) matrices, the other graphs are zero. We have

$$\Sigma_a^{nm}(p)=\delta^{nm}\Sigma_a(p), \tag{29}$$

$$\Sigma_b^{nm}(p)=\mathrm{tr}(I)\delta^{nm}\Sigma_a(p), \tag{30}$$

$$\Sigma_c^{nm}(p)=[T^aT_a]^{nm}\Sigma_a(p)_{\lambda_1\to\lambda_2}, \tag{31}$$

where again the subscripts are in a strict correspondence with the diagrams mentioned and

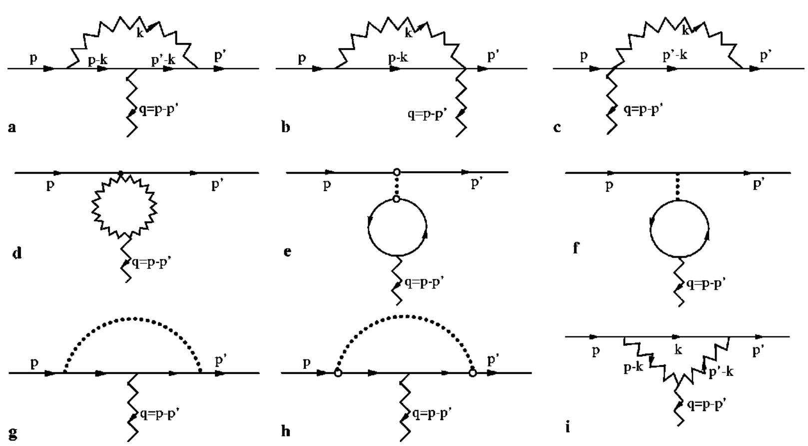

FIG. 4. Corrections to the CS-matter field trilinear vertex.

$$\Sigma_a(p) = -i\frac{\lambda_1}{2}\int \frac{d^3k}{(2\pi)^3}\Delta(k) = \frac{\lambda_1}{2}\int^{\Lambda_0}\frac{d^3k}{(2\pi)^3}\frac{1}{k^2-m^2+i\epsilon}, \tag{32}$$

where Λ_0 is an ultraviolet cutoff in the spatial part of the above integral. The integral is linearly divergent, but this divergence could be absorbed by a mass renormalization.

Let us now look at the CS field polarization tensor. The nonvanishing graphs are shown in Figs. 3(d) and 3(e). Up to a group factor, they give the same result as in the Abelian case [4]

$$\Pi^{\mu\nu,ab}(q) = \frac{ig^2}{8\pi}\mathrm{tr}\,(T^aT^b)(q^2g^{\mu\nu}-q^\mu q^\nu)\Pi(q^2), \tag{33}$$

where

$$\Pi(q^2) = \int_0^1 dx\frac{1-4x+4x^2}{[m^2-q^2x(1-x)]^{(1/2)}} \approx \frac{1}{3m}\left[1+\frac{q^2}{20m^2}\right], \tag{34}$$

where the approximated result is valid for m large compared with the momentum q. It is a purely relativistic quantum field theory contribution.

Consider now the corrections to the trilinear CS-matter field vertex as shown in Fig. 4. Graphs 4(e)–4(h) vanish due to the oddness of the integrand. Although not so obvious, graph 4(d) also vanishes. Since the integrand is k_0 independent, this result follows by first regularizing the k^0 part of the integral. More details on this will be given later, when discussing the two body scattering amplitude. Graph 4(a) has the analytic expression

$$\Gamma^{\mu,b}_{(a)nm}(p,p') = [T^cT^bT_c]_{nm}\Gamma^\mu_{(a)}(p,p'), \tag{35}$$

where

$$\Gamma^\mu_{(a)}(p,p') = \frac{-g^3}{\Theta}\int\frac{d^3k}{(2\pi)^3}\left[\frac{(2p-k)^\sigma\varepsilon_{\sigma\rho\lambda}\overline{k^\lambda}(2p'-k)^\rho(p+p'-k)^\mu}{\mathbf{k}^2[(p-k)^2-m^2+i\epsilon][(p'-k)^2-m^2+i\epsilon]}\right]. \tag{36}$$

In the low momentum regime, this expression is easily integrated and we get

$$\Gamma^0_{(a)}(p,p') = \frac{ig^3}{4\pi\Theta m}\varepsilon_{ij}p^iq^j, \tag{37}$$

$$\Gamma^l_{(a)}(p,p') = \frac{-ig^3}{8\pi\Theta}\left[\varepsilon_{ij}\frac{p^iq^j}{m}\left(\frac{p^l+p'^l}{2m}\right) - 2\varepsilon^{il}q_i\left(1+\frac{\mathbf{p}^2}{12m^2}[2+\cos(\theta)]\right)\right], \tag{38}$$

where $q=p-p'$.

Graphs 4(b) and 4(c) have the expressions

$$\Gamma^{\mu,a}_{(b)nm}(p,p') = [(T^aT^c+T^cT^a)T_c]_{nm}\Gamma^\mu_{(b)}(p,p'),$$
$$\Gamma^{\mu,a}_{(c)nm}(p,p') = [T_b(T^aT^b+T^bT^a)]_{mn}\Gamma^\mu_{(c)}(p,p'), \tag{39}$$

where

$$\Gamma^\mu_{(b)}(p,p') = \frac{g^3}{\Theta}\int\frac{d^3k}{(2\pi)^3}\left[\frac{(2p-k)^\sigma\varepsilon_{\sigma\rho\lambda}\overline{k^\lambda}g^{\rho\mu}}{\mathbf{k}^2[(p-k)^2-m^2+i\epsilon]}\right], \tag{40}$$

$$\Gamma^\mu_{(c)}(p,p') = \frac{g^3}{\Theta}\int\frac{d^3k}{(2\pi)^3}\left[\frac{(2p'-k)^\sigma\varepsilon_{\sigma\rho\lambda}\overline{k^\lambda}g^{\rho\mu}}{\mathbf{k}^2[(p'-k)^2-m^2+i\epsilon]}\right]. \tag{41}$$

Performing the integrals, we obtain

$$\Gamma^0_{(b)}(p,p') = \Gamma^0_{(c)}(p,p') \approx 0 \tag{42}$$

$$\Gamma^l_{(b)}(p,p') + \Gamma^l_{(c)}(p,p') = \frac{ig^3}{4\pi\Theta}\varepsilon_{ij}g^{jl}q^if(\mathbf{p}^2,m^2), \tag{43}$$

where

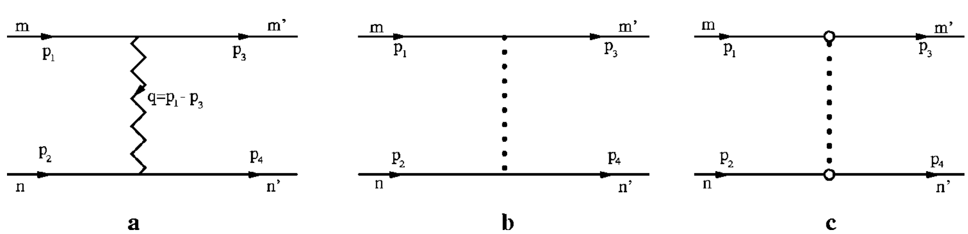

FIG. 5. Tree approximation to the scattering.

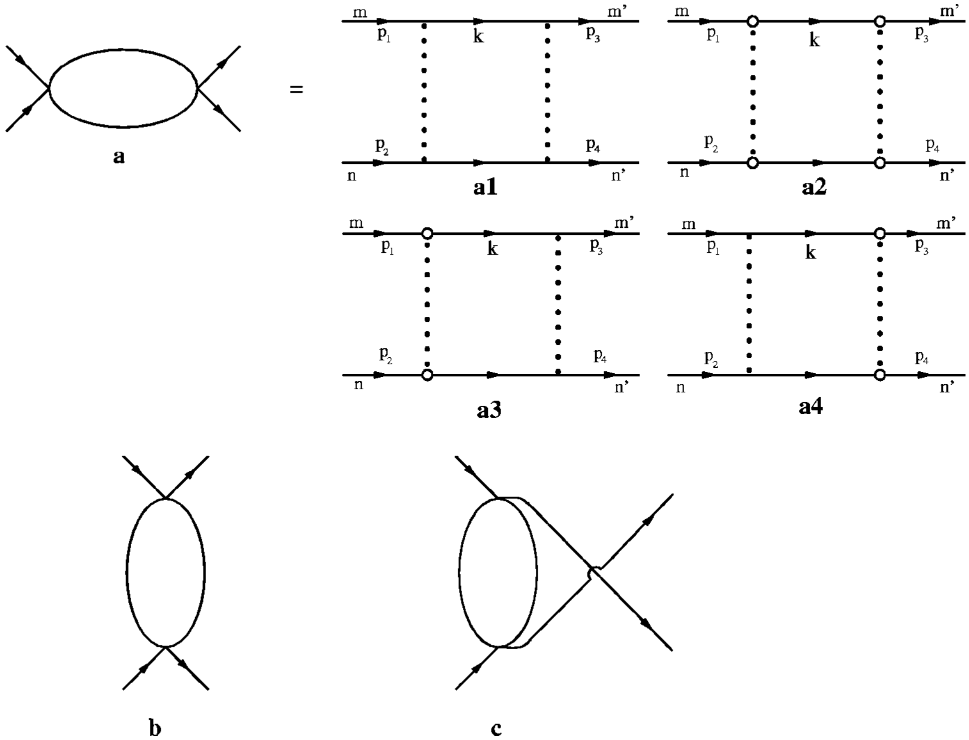

FIG. 6. λ's second order contributions to the scattering.

$$f(\mathbf{p}^2,m^2)=\frac{\sqrt{m^2+\mathbf{p}^2}}{\sqrt{m^2}+\sqrt{m^2+\mathbf{p}^2}}\approx\frac{1}{2}+\frac{\mathbf{p}^2}{8m^2}. \qquad (44)$$

We postpone the computation of the graph 4(i) until the discussion of the two body scattering, to be done shortly.

Besides the two body scattering amplitude, to conclude our study of the one loop divergences we still have to look at the corrections to the trilinear CS field vertex. There is just one graph consisting of a closed loop of matter field propagators which, by power counting, is logarithmically divergent (the other graphs cancel, as shown in [14]). However, as it is easily checked, it is in fact convergent by symmetric integration. We will not explicitly compute this diagram since, up to one loop, it does not contribute to the scattering; we just want to remark that, together with the vacuum polar-

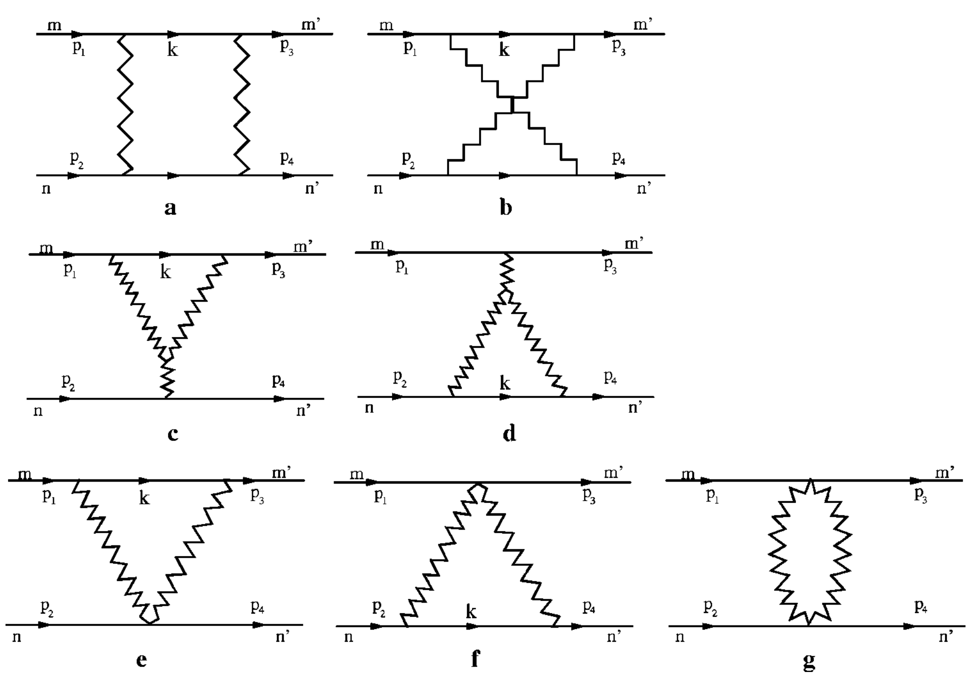

FIG. 7. Graphs contributing to the scattering having only CS-matter field vertices.

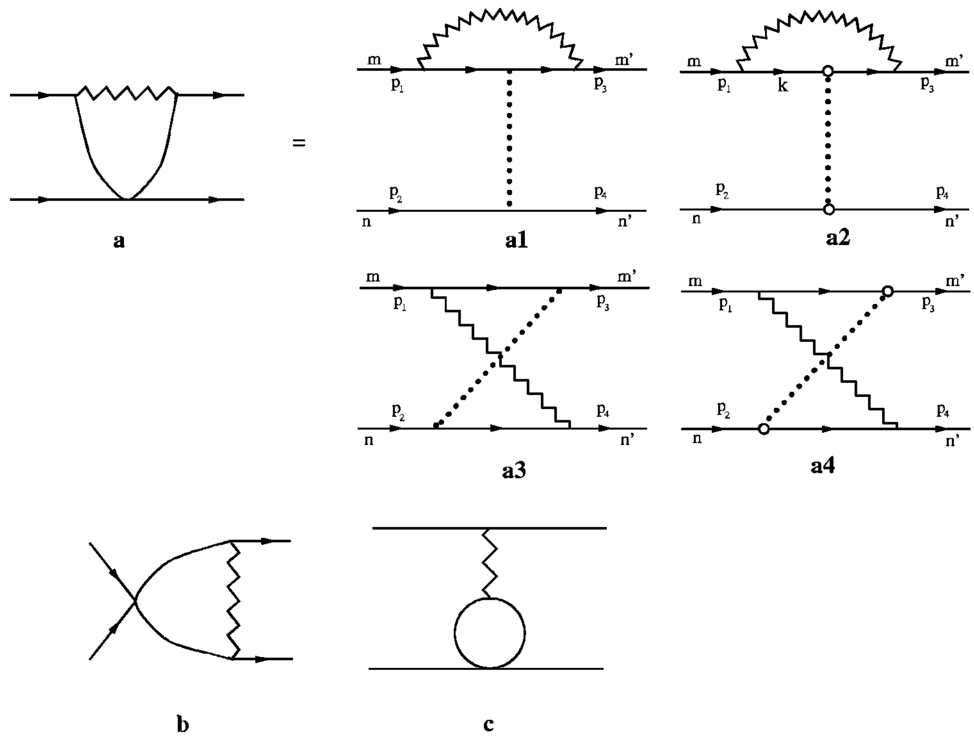

FIG. 8. Graphs admixing the quadrilinear scalar and trilinear CS-matter field vertices.

ization calculated before and the one loop CS field four point function, it implies that a Yang-Mills kinetic term

$$\frac{1}{4}\,\frac{g^2}{24\pi m}\,\mathrm{tr}[F^{\mu\nu}F_{\mu\nu}] \tag{45}$$

is induced in the effective low momentum Lagrangian. So, up to this point, only a trivial mass renormalization of the matter field is necessary.

We are now ready to pursue our study of the two body scattering process. In our computations we will work in the center of mass frame and shall retain terms up to order $|\mathbf{p}|^2/m^2 \approx |\mathbf{p}|^4/\Lambda^4 \approx \Lambda^4/m^4$, where $\mathbf{p}$ is the momentum of the incoming particles and Λ the intermediary cutoff which separates the regions of low and high momenta in the spatial part of the Feynman integrals.

In the tree approximation, the contributing graphs are those shown in Fig. 5. We get

$$\mathcal{M}_{tree}(\theta) = -\frac{\lambda_1[I\otimes I]+\lambda_2[T^a\otimes T_a]}{2} - i(8\pi)\Omega\,\omega_p \cot(\theta/2). \tag{46}$$

Of course, we may adjust the coupling constants to correctly reproduce the nonrelativistic result. Prior to that, however, we will examine the one loop contributions which are listed in Figs. 6, 7 and 8.

Let us begin by looking at the 2nd order (in λ_1 and λ_2) graphs. The box diagrams, Figs. 6(a1)–6(a4), furnish

$$\mathcal{M}_{\lambda^2(a)}(\theta) = \frac{1}{4}[-\lambda_1^2 I\otimes I - 2\lambda_1\lambda_2 T^a\otimes T_a - \lambda_2^2 T^a T^b \otimes T_a T_b] I^{(1)}(\theta), \tag{47}$$

where

$$I^{(1)}(\theta) = -i\int \frac{d^3k}{(2\pi)^3}\Delta(k)\Delta(p_1+p_2-k). \tag{48}$$

We now detail the calculation of the above expression; to illustrate the general procedure we shall follow in the evaluation of the contributing graphs. First we integrate in k^0 getting

$$I^{(1)}(\theta) = \frac{1}{32\pi^2}\int_0^\infty d(\mathbf{k})^2 \int_0^{2\pi} d\alpha \frac{1}{w_k}\,\frac{1}{\mathbf{p}^2-\mathbf{k}^2+i\epsilon},$$

where $w_k = \sqrt{\mathbf{k}^2+m}$. The angular α integration is trivial and gives 2π. In order to facilitate the taking of the nonrelativistic limit it is useful to introduce an auxiliary cutoff Λ, satisfying $|\mathbf{p}| \ll \Lambda \ll m$, which separates the integral in two regions of *low* $(0 \leqslant \mathbf{k}^2 \leqslant \Lambda^2)$ and *high* $(\mathbf{k}^2 \geqslant \Lambda^2)$ loop momentum. In the *low* part of the integral the integrand is expanded in power of $1/m$ whereas in the *high* part it is approximated by a Taylor expansion around $\mathbf{p}=0$. We thus arrive at

$$I^{(1)}(\theta) = I^{(1)}_{low}(\theta) + I^{(1)}_{high}(\theta), \tag{49}$$

$$I^{(1)}_{low}(\theta)=\frac{1}{16\pi}\int_0^{\Lambda}d(\mathbf{k})^2\frac{1}{w_k}\frac{1}{\mathbf{p}^2-\mathbf{k}^2+i\epsilon} \tag{50}$$

$$=\frac{-1}{16\pi m}\left\{\left(1-\frac{\mathbf{p}^2}{2m^2}\right)\left[\log\left(\frac{\Lambda^2}{\mathbf{p}^2}\right)+i\pi\right]-\frac{\mathbf{p}^2}{\Lambda^2}-\frac{\mathbf{p}^4}{2\Lambda^4}-\frac{\Lambda^2}{2m^2}+\frac{3\Lambda^4}{16m^4}\right\}, \tag{51}$$

$$I^{(1)}_{high}(\theta)=\frac{1}{16\pi}\int_{\Lambda}^{\infty}d(\mathbf{k})^2\frac{1}{w_k}\frac{1}{\mathbf{p}^2-\mathbf{k}^2+i\epsilon} \tag{52}$$

$$=\frac{1}{16\pi m}\left\{\left(1-\frac{\mathbf{p}^2}{2m^2}\right)\log\left(\frac{\Lambda^2}{4m^2}\right)-\frac{\mathbf{p}^2}{2m^2}-\frac{\mathbf{p}^2}{\Lambda^2}-\frac{\mathbf{p}^4}{2\Lambda^4}-\frac{\Lambda^2}{2m^2}+\frac{3\Lambda^4}{16m^4}\right\}, \tag{53}$$

so that

$$I^{(1)}(\theta)=\frac{-1}{16\pi m}\left\{\left(1-\frac{\mathbf{p}^2}{2m^2}\right)\left[\log\left(\frac{4m^2}{\mathbf{p}^2}\right)+i\pi\right]+\frac{\mathbf{p}^2}{2m^2}\right\}. \tag{54}$$

Notice that if we consider the *low* part of the above result and reinterpret Λ as the nonrelativistic Λ_{NR} cutoff then the leading contribution to Eq. (51) is the same as the result (17) from Sec. II. Here, however, a counterterm is automatically provided by the contribution of the *high* energy part and, consequently, the final result (54) is finite. In the effective field theory program [6] the high energy parts, which are only polynomials in $\mathbf{p}^2$, are associated to new interactions to be introduced in the nonrelativistic Lagrangian.

Following the same steps described above, the sum of the remaining graphs, Figs. 6(b) and 6(c), give

$$\mathcal{M}_{\lambda^2(bc)}(\theta)=-\frac{1}{64\pi m}\left[\left(-5\lambda_1^2+\frac{3}{2}\lambda_1\lambda_2-\frac{3}{16}\lambda_2^2\right)I\otimes I+\left(-4\lambda_1\lambda_2+\frac{1}{2}\lambda_2^2\right)T^a\otimes T^a\right]\left(2-\frac{\mathbf{p}^2}{3m^2}\right)$$
$$-\frac{1}{64\pi m}\left[\left(-3\lambda_1^2+\frac{3}{2}\lambda_1\lambda_2+\frac{3}{16}\lambda_2^2\right)I\otimes I-\frac{1}{2}\lambda_2^2T^a\otimes T^a\right]\frac{\mathbf{p}^2}{3m^2}\cos\theta. \tag{55}$$

As expected, the above result comes essentially from the high energy part of the corresponding integrals. Let us now examine the graphs involving the CS field which are listed in Fig. 7. The graphs in the first row, the direct box and twisted box diagrams, are given respectively by

$$\mathcal{M}_{g^4(a)}(\theta)=-ig^4[T^aT^c\otimes T_aT_c]\int\frac{d^3k}{(2\pi)^3}\{\Delta(k)\Delta(p_1+p_2-k)(p_1+k)^{\mu}D_{\sigma\mu}(k-p_1)(2p_2+p_1-k)^{\sigma}[(p_3+k)^{\nu}D_{\nu\rho}(k-p_3)$$
$$\times(p_2+p_1+p_4-k)^{\rho}]\},$$

$$\mathcal{M}_{g^4(b)}(\theta)=-ig^4[T^aT^c\otimes T_cT_a]\int\frac{d^3k}{(2\pi)^3}\{\Delta(k)\Delta(k+p_2-p_3)(p_1+k)^{\mu}D_{\mu\sigma}(p_1-k)(k+p_2-p_3+p_4)^{\sigma}$$
$$\times[(2p_2-p_3+k)^{\nu}D_{\nu\rho}(p_3-k)(k+p_3)^{\rho}]\}. \tag{56}$$

Performing the integrals one finds that the low energy part, after the reinterpretation of the intermediary cutoff, has a logarithmic divergence which is canceled by the contribution from the high energy part. The final result for the sum of these graphs is

$$\mathcal{M}_{g^4(ab)}(\theta)=\frac{-g^4m}{2\pi\Theta^2}[T^aT^c\otimes T_aT_c]\left\{2\left(1+\frac{\mathbf{p}^2}{2m^2}\right)[\log[2(1-\cos\theta)]+i\pi]-2\cos\theta\left[\log[2(1-\cos\theta)]\right.\right.$$
$$\left.\left.-\log\left(\frac{4m^2}{\mathbf{p}^2}\right)\right]\frac{\mathbf{p}^2}{m^2}-\frac{\mathbf{p}^2}{m^2}(1+\cos\theta)\right\}+\frac{g^4m}{4\pi\Theta^2}[T^a\otimes T_a]\left(2(1+\cos\theta)\frac{\mathbf{p}^2}{m^2}\right). \tag{57}$$

The next set of diagrams in Fig. 7 needs special care since they contain a genuine ultraviolet divergence of the relativistic theory. In fact they may have divergences in both k_0 and $\mathbf{k}$ parts of the loop momentum integral. We found that they are naturally grouped in two sets which have distinct properties. We shall discuss each of them separately.

The graphs of the first set, Figs. 7(c) and 7(d), are potentially more dangerous for, because of the form taken by the CS propagator, the k^0 integration is not well defined. We found that, as suggested in [14], this difficulty can be circumvented by first regularizing the k_0 integral. For practical purpose we will introduce an additional cutoff so that

$$\int dk_0 f(k_0) \to \int_{-L}^{L} f(k_0), \tag{58}$$

but the final result actually does not depend on the regularization one chooses. It turns out that the spatial integral multiplying the k_0 integral vanishes. To see how this happens, consider the graph 7(c) whose analytic expression is

$$\mathcal{M}_{g^4(c)}(\theta) = -g^4 \Theta [\varepsilon_{bac} T^b \otimes T^c T^a] D_{\sigma'\sigma}(q) \varepsilon^{\sigma'\mu'\nu'} (p_2+p_4)^\sigma \int \frac{d^3k}{(2\pi)^3} [(k+p_3)^\nu \Delta(k)(k+p_1)^\mu] D_{\mu'\mu}(k-p_1) D_{\nu\nu'}(k-p_3). \tag{59}$$

After some arrangement, the above expression can be rewritten as

$$\mathcal{M}_{g^4(c)}(\theta) = \frac{-2g^4}{\Theta^2} [\varepsilon_{bac} T^b \otimes T^c T^a] \int \frac{d^2\mathbf{k}}{(2\pi)^2} \frac{[\mathbf{q}\wedge\mathbf{k} - \mathbf{p}_1 \wedge \mathbf{p}_3]}{[(\mathbf{k}-\mathbf{p}_1)^2][(\mathbf{k}-\mathbf{p}_3)^2][\mathbf{q}^2]} T_0, \tag{60}$$

where

$$T_0 = \int_{-L}^{L} \frac{dk^0}{(2\pi)} \frac{2w_q(k^0+w_q)[\mathbf{q}\wedge\mathbf{k}] + (k^0+w_q)^2 [\mathbf{p}_1\wedge\mathbf{p}_3]}{k_0^2 - w_k^2 + i\epsilon}. \tag{61}$$

For L large enough, we obtain

$$T_0 = [\mathbf{q}\wedge\mathbf{k}] \frac{w_p^2}{w_k} + [\mathbf{p}_1\wedge\mathbf{p}_3] \frac{w_p^2 + w_k^2}{2w_k} + \frac{L}{\pi} [\mathbf{p}_1\wedge\mathbf{p}_3]. \tag{62}$$

Notice now that the spatial integral multiplying the divergent piece in T_0 is

$$\int \frac{d^2\mathbf{k}}{(2\pi)^2} \frac{(\mathbf{k}-\mathbf{p_1})\wedge(\mathbf{k}-\mathbf{p_3})}{[(\mathbf{k}-\mathbf{p}_1)^2][(\mathbf{k}-\mathbf{p}_3)^2]} = 0, \tag{63}$$

so that no counterterm will be needed if we agree to eliminate the cutoff L only at the end of the calculation. Proceeding in this way and making the nonrelativistic approximation we arrive at

$$\mathcal{M}_{g^4(cd)}(\theta) = -\frac{g^4 m}{4\pi\Theta^2} [T^a \otimes T_a] \left\{ 2 + \left[\frac{11}{2} + 3\cos\theta\right] \frac{\mathbf{p}^2}{m^2} + \left(2 + [1 - 2\cos\theta] \frac{\mathbf{p}^2}{m^2}\right) \left[\log\left(\frac{4m^2}{\mathbf{p}^2}\right) - [\log[2(1-\cos\theta)]]\right]\right\} \tag{64}$$

for the sum of the graphs 7(c) and 7(d).

Similarly to the calculation for the 7(c) graph, each one of the graphs 7(e)–7(g) presents a linear divergence in L. This divergence is however eliminated when we sum the contributions so that the final result is

$$\begin{aligned}\mathcal{M}_{g^4(efg)}(\theta) = {} & \frac{-g^4 m}{2\pi\Theta^2} [T^a T^c \otimes T_a T_c] \left\{ -2 + (2+\cos\theta) \frac{\mathbf{p}^2}{m^2} + \left(2 + [1-2\cos\theta] \frac{\mathbf{p}^2}{m^2}\right) \left[\log\left(\frac{4m^2}{\mathbf{p}^2}\right) - [\log[2(1-\cos\theta)]]\right]\right\} \\ & + \frac{g^4 m}{4\pi\Theta^2} [T^a \otimes T_a] \left\{ -2 + (2+\cos\theta) \frac{\mathbf{p}^2}{m^2} + \left(2 + [1-2\cos\theta] \frac{\mathbf{p}^2}{m^2}\right) \left[\log\left(\frac{4m^2}{\mathbf{p}^2}\right) - [\log[2(1-\cos\theta)]]\right]\right\} \\ & - \frac{3g^4 m}{16\pi\Theta^2} [I\otimes I] \frac{\Lambda_0}{m},\end{aligned} \tag{65}$$

where Λ_0 in an ultraviolet cutoff introduced in the spatial part of the integral. The divergent term proportional to this cutoff can be removed by a redefinition of the coupling constant λ_1. After this, the final result for the sum of the graphs in Fig. 7 is

$$\mathcal{M}_{g^4}(\theta)=\frac{-g^4m}{2\pi\Theta^2}[T^aT^c\otimes T_aT_c]\left\{2\left(1+\frac{\mathbf{p}^2}{2m^2}\right)\left[\log\left(\frac{4m^2}{\mathbf{p}^2}\right)+i\pi\right]+\frac{\mathbf{p}^2}{m^2}\right\}-\frac{g^4m}{4\pi\Theta^2}[T^a\otimes T_a]\frac{3}{2}\frac{\mathbf{p}^2}{m^2}. \tag{66}$$

We still have to incorporate to our calculation the contributions of graphs with vacuum polarization and vertex corrections. They do not exist in the nonrelativistic theory of the previous section and their contribution come entirely from the *high* energy part. Using Eq. (33), the insertions of vacuum polarization graphs give

$$\mathcal{M}_P(\theta)=\frac{g^4m}{4\pi\Theta^2}[T^a\otimes T_a]\left\{\frac{1}{3}+\frac{7}{15}\frac{\mathbf{p}^2}{m^2}+\frac{1}{5}\frac{\mathbf{p}^2}{m^2}\cos\theta\right\}, \tag{67}$$

whereas, using Eqs. (37), (38), and (43), the vertex corrections produce

$$\mathcal{M}_V(\theta)=-\frac{g^4m}{4\pi\Theta^2}[T^a\otimes T_a]\left\{\frac{1}{6}\frac{\mathbf{p}^2}{m^2}+\frac{1}{3}\frac{\mathbf{p}^2}{m^2}\cos\theta\right\}. \tag{68}$$

At last, there are some contributions from graphs that admix the quadrilinear scalar vertex and the CS–matter field vertex. They are shown in Fig. 8 and give the result

$$\mathcal{M}_{\lambda g^2}(\theta)=-\frac{ig^2}{8\pi\Theta}\left[\frac{3}{4}\left(\lambda_1+\frac{\lambda_2}{4}\right)I\otimes I+\left(\lambda_1+\frac{3}{4}\lambda_2\right)T^a\otimes T_a\right]\frac{\mathbf{p}^2}{m^2}\sin\theta. \tag{69}$$

In the Abelian situation the corresponding amplitude is canceled by its exchanged particle partner. Here, because of the nonabelian structure, even after symmetrization the result is nonvanishing.

Our one loop calculation is now completed. Collecting all the results above, the total one loop amplitude (without symmetrization) is given by

$$\begin{aligned}\mathcal{M}_{1loop}=&\frac{-1}{64\pi m}\left[\left(-\lambda_1^2-\frac{3}{16}\lambda_2^2\right)I\otimes I+\left(-\frac{1}{2}\lambda_2^2-2\lambda_1\lambda_2\right)T^a\otimes T_a\right]\left\{\left(1-\frac{\mathbf{p}^2}{2m^2}\right)\left[\log\left(\frac{4m^2}{\mathbf{p}^2}\right)+i\pi\right]+\frac{\mathbf{p}^2}{2m^2}\right\}\\&-\frac{1}{64\pi m}\left[\left(-5\lambda_1^2+\frac{3}{2}\lambda_1\lambda_2-\frac{3}{16}\lambda_2^2\right)I\otimes I+\left(-4\lambda_1\lambda_2+\frac{1}{2}\lambda_2^2\right)T^a\otimes T_a\right]\left(-\frac{\mathbf{p}^2}{3m^2}\right)\\&-\frac{1}{64\pi m}\left[\left(-3\lambda_1^2+\frac{3}{2}\lambda_1\lambda_2+\frac{3}{16}\lambda_2^2\right)I\otimes I-\left(\frac{1}{2}\lambda_2^2\right)T^a\otimes T_a\right]\frac{\mathbf{p}^2}{3m^2}\cos\theta-\frac{g^4m}{2\pi\Theta^2}[T^aT^c\otimes T_aT_c]\\&\times\left\{2\left(1+\frac{\mathbf{p}^2}{2m^2}\right)\left[\log\left(\frac{4m^2}{\mathbf{p}^2}\right)+i\pi\right]+\frac{\mathbf{p}^2}{m^2}\right\}-\frac{g^4m}{4\pi\Theta^2}[T^a\otimes T_a]\left\{\frac{18}{15}\frac{\mathbf{p}^2}{m^2}+\frac{2}{15}\frac{\mathbf{p}^2}{m^2}\cos\theta\right\}-\frac{ig^2}{8\pi\Theta}\left[\frac{3}{4}\left(\lambda_1+\frac{\lambda_2}{4}\right)I\otimes I\right.\\&\left.+\left(\lambda_1-\frac{3}{4}\lambda_2\right)T^a\otimes T_a\right]\frac{\mathbf{p}^2}{m^2}\sin\theta.\end{aligned} \tag{70}$$

We are now in a position to compare the results of this section with the ones stated in the preceding section. Before doing that we will need to adjust some normalization factors. These come from the normalization of the relativistic one particle states, $\langle\mathbf{p}'|\mathbf{p}\rangle=2\omega_p\delta(\mathbf{p}'-\mathbf{p})$, whereas the nonrelativistic theory does not have the $2w_p$ factor. Another factor to take into consideration is $f=\sqrt{\omega_p/m}$ which comes from the different expressions used for the relativistic and nonrelativistic velocities. Altogether, we need to multiply the relativistic expression by the kinematic factor

$$f\left(\frac{1}{\sqrt{2\omega_p}}\right)^4=\frac{1}{4m^2}\left[1-\frac{3\mathbf{p}^2}{4m^2}+\cdots\right]. \tag{71}$$

Thus, to leading order in $\mathbf{p}/m$, we have

$$\mathcal{M}^{dom}(\theta) = -\frac{1}{2}\left(\frac{\lambda_{eff}}{4m^2}\right) - i\frac{2\pi}{m}\Omega\cot(\theta/2) + \frac{m}{16\pi}\left[\left(\frac{\lambda_{eff}}{4m^2}\right)^2 - \frac{16\pi^2}{m^2}\Omega^2\right] \times \left\{\log\left[\frac{4m^2}{\mathbf{p}^2}\right] + i\pi\right\}, \tag{72}$$

where $\lambda_{eff} = \lambda_1[I\otimes I] + \lambda_2[T^a\otimes T_a]$. As remarked after Eq. (54) and explicit in Eqs. (51) and (53), the low energy part of this formula coincides with the nonrelativistic result, after the identification of the intermediary with the nonrelativistic cutoff. In our calculation, however, the *high* part provides the necessary counterterm to the *low* part and the final result becomes automatically finite.

To restore the conformal invariance of the tree approximation, eliminating the log term and obtaining the same result as in the expansion of the exact amplitude one must choose $\lambda_1 = 0$ and $\lambda_2 = 8mg^2/(|\Theta|)$. At these values of the renormalized quartic self-interaction there are subdominant terms in Eq. (70) that survive, namely,

$$\mathcal{M}^{sub} = \frac{i\pi}{2m}\left[\Omega\cot(\theta/2) - i\frac{3}{4}\left|\Omega\right|\right]\frac{\mathbf{p}^2}{m^2} - \frac{g^4}{4\pi m\Theta^2}\left[\frac{3}{16}I\otimes I - \frac{1}{2}T^a\otimes T_a\right]\frac{\mathbf{p}^2}{m^2}\left(\log\left[\frac{4m^2}{\mathbf{p}^2}\right] + i\pi\right) - \frac{g^4}{4\pi m\Theta^2}\left\{\left[\frac{1}{16}I\otimes I + \frac{2}{15}T^a\otimes T_a\right]\frac{\mathbf{p}^2}{m^2} + \left[\frac{1}{16}I\otimes I - \frac{2}{15}T^a\otimes T_a\right]\frac{\mathbf{p}^2}{m^2}\cos\theta\right\} \pm \frac{ig^4}{4\pi m\Theta|\Theta|}\left[\frac{3}{16}I\otimes I - \frac{3}{4}T^a\otimes T_a\right]\frac{\mathbf{p}^2}{m^2}\sin\theta \tag{73}$$

and represent relativistic corrections to the non-Abelian AB scattering. These terms break conformal invariance which is therefore only a property of the leading approximation. The first row of the above formula are corrections of the tree level and are partially of kinematical rise and partially due to the energy dependence of the relativistic amplitude Eq. (46). The other terms, proportional to g^4 are absent in the nonrelativistic Aharonov-Bohm scattering which contains only odd powers of g^2 [11]. In an effective low momentum Lagrangian they would correspond to derivative quartic self-couplings of the matter field ϕ. The subleading corrections change also the nature of the effective AB potential: because of vacuum polarization, this potential is not strictly localized at the origin and the AB effect, considered as the scattering by an impenetrable flux tube, only exists in a quantum mechanical, first quantized level.

ACKNOWLEDGMENTS

This work was partially supported by Conselho Nacional de Desenvolvimento Científico e Tecnológico (CNPq) and Coordenação de Aperfeiçoamento de Pessoal de Nível Superior (Capes).

[1] Y. Aharonov and D. Bohm, Phys. Rev. **115**, 485 (1959).
[2] E. L. Feinberg, Sov. Phys. Usp. **5**, 7530 (1963); E. Corinaldesi and F. Rafaeli, Am. J. Phys. **46**, 1185 (1978); K. M. Purcell and W. C. Henneberger, *ibid.* **46**, 1255 (1978).
[3] O. Bergman and G. Lozano, Ann. Phys. (N.Y.) **229**, 416 (1994).
[4] M. Gomes, J. M. C. Malbouisson, and A. J. da Silva, Phys. Lett. A **236**, 373 (1997); M. Boz, V. Fainberg, and N. K. Pak, Ann. Phys. (N.Y.) **246**, 347 (1996).
[5] H. O. Girotti, M. Gomes, J. R. S. Nascimento, and A. J. da Silva, Phys. Rev. D **56**, 3623 (1997); M. Gomes and A. J. da Silva, *ibid.* **57**, 3579 (1998).
[6] S. Weinberg, *The Quantum Theory of Fields* (Cambridge University Press, Cambridge, England, 1995); K. G. Wilson, Phys. Rev. B **4**, 3174 (1971); G. P. Lepage *et al.*, Phys. Rev. D **46**, 4052 (1992).
[7] C. R. Hagen, Phys. Rev. D **56**, 2250 (1997).
[8] Ph. de Souza Gerbert, Phys. Rev. D **40**, 1346 (1989); M. Alford, J. Marc-Russel, and F. Wilczek, Nucl. Phys. **B337**, 695 (1990).
[9] T. T. Wu and C. N. Yang, Phys. Rev. D **12**, 3845 (1975).
[10] P. A. Horváthy, Phys. Rev. D **33**, 407 (1986); T. Lee and P. Oh, Ann. Phys. (N.Y.) **235**, 413 (1994); C. Hagen, Phys. Rev. D **31**, 848 (1985).

[11] D. Bak and O. Bergman, Phys. Rev. D **51**, 1994 (1995).

[12] G. Amelino-Camelia and D. Bak, Phys. Rev. Lett. B **343**, 231 (1995); C. Lee, Int. J. Mod. Phys. A **12**, 1033 (1997); D. Bak, R. Jackiw, and S.-Y. Pi, Phys. Rev. D **49**, 6778 (1994).

[13] First applications of the (CS) term to physics are in J. F. Schonfeld, Nucl. Phys. **B185**, 157 (1981); S. Deser, R. Jackiw, and S. Templeton, Ann. Phys. (N.Y.) **140**, 372 (1982).

[14] F. Ferrari and I. Lazzizzera, Int. J. Mod. Phys. A **13**, 1773 (1998).

[15] In a covariant Landau gauge, the non-Abelian CS theory was discussed by W. Chen, G. W. Semenoff, and Y. S. Wu, Phys. Rev. D **46**, 5521 (1992); G. Amelino-Camelia, I. I. Kogan, and R. J. Szabo, Nucl. Phys. **B480**, 413 (1996); G. Giavarini, C. P. Martin, and F. Ruiz Ruiz, *ibid.* **B381**, 222 (1992).